

Published in final edited form as:

Infect Genet Evol. 2011 March ; 11(2): 391–398. doi:10.1016/j.meegid.2010.11.010.

High-throughput molecular diagnosis of circumsporozoite variants VK210 and VK247 detects complex *Plasmodium vivax* infections in malaria endemic populations in Papua New Guinea

Cara N. Henry-Halldin^a, Daphne Sepe^b, Melinda Susapu^b, David T. McNamara^a, Moses Bockarie^a, Christopher L. King^a, and Peter A. Zimmerman^{a,*}

^aCenter for Global Health and Diseases, Case Western Reserve University, Wolstein Research Building, Room 4-125, 2103 Cornell Rd., Cleveland, OH 44106, United States

^bPapua New Guinea Institute of Medical Research, PO Box 378, Madang, Madang 511, Papua New Guinea

Abstract

Malaria is endemic in lowland and coastal regions of Papua New Guinea (PNG), and is caused by *Plasmodium falciparum*, *Plasmodium vivax*, *Plasmodium malariae* and *Plasmodium ovale*. Infection by *P. vivax* is attributed to distinct strains, VK210 and VK247, which differ in the sequence of the circumsporozoite protein (*pvcs*). Here, based upon sequence polymorphisms in *pvcs*, we developed a post-PCR ligation detection reaction-fluorescent microsphere assay (LDR-FMA) to distinguish these *P. vivax* strains. This diagnostic assay was designed to detect the presence of both VK210 and VK247 *P. vivax* strains simultaneously in a high-throughput 96-well format. Using this assay, we analyzed human blood samples from the Wosera ($n = 703$) and Mugil ($n = 986$) regions to evaluate the prevalence of these *P. vivax* strains. VK210 and VK247 strains were found in both study sites. In the Wosera, single infections with VK210 strain were observed to be most common (41.7%), followed by mixed-strain (36.8%) and VK247 single-strain infections (21.5%). Similarly, in Mugil, VK210 single-strain infections were most common (51.6%), followed by mixed-strain (34.4%) and VK247 single-strain infections (14%). These results suggest that the distribution of *P. vivax* infections was similar between the two study sites. Interestingly, we observed a non-random distribution of these two *P. vivax* strains, as mixed-strain infections were significantly more prevalent than expected in both study sites (Wosera and Mugil χ^2 p -value < 0.001). Additionally, DNA sequence analysis of a subset of *P. vivax* infections showed that no individual *pvcs* alleles were shared between the two study sites. Overall, our results illustrate that PNG malaria-endemic regions harbor a complex mixture of *P. vivax* strains, and emphasize the importance of malaria control strategies that would be effective against a highly diverse parasite population.

Keywords

Malaria; *Plasmodium vivax*; Circumsporozoite protein; VK210; VK247; Papua New Guinea

1. Introduction

Of the four human malaria parasites, *Plasmodium vivax* is the most widespread species currently found in limited parts of Africa, parts of Central and South America as well as the

Middle East, and most of Central, Northeast, South, and Southeast Asia, including the Pacific Islands (Carter and Mendis, 2002; Mendis et al., 2001). In 2009, an estimated 2.85 billion people were at risk of *P. vivax* infection, which causes approximately 80 million clinical cases each year (Guerra et al., 2006, 2010; Mendis et al., 2001). *P. vivax* infection begins with the injection of sporozoites into the human host by an infectious mosquito. Sporozoites then migrate to the liver, where they invade hepatocytes and proceed through asexual exo-erythrocytic development. Infected hepatocytes develop either into schizonts, to begin the blood stage development of malaria infection, or into the dormant hypnozoite stage. Hypnozoites can become reactivated and proceed to schizogony many months after initial sporozoite inoculation to cause a relapse infection (Krotoski et al., 1986). As a result, the complexity of *P. vivax* blood stage infections are likely to be high because they may receive contribution from as many as four sources; primary infection, reinfection, recrudescence from surviving blood stage parasites, or relapse caused by an activated hypnozoite.

Consistent with observations from other malaria parasite species, the *P. vivax* sporozoite expresses an abundant surface protein, the circumsporozoite protein (pvcsp) (Arnot et al., 1985; Rosenberg et al., 1989). Earlier studies showed that the central region of *pvcsp* consists of 15–19 repeats, each 27 bp in length (encoding nine amino acids), with polymorphism that leads to classification as two different variants, VK210 and VK247 (Rosenberg et al., 1989). The VK210 repeat consists of various multiples and combinations of the GDRA[D/A/P]GQPA amino acid motif. The terminal repeat of the VK210 variant has shown to be consistently comprised of the GDRAAGQPA amino acid motif, which is immediately followed by a conserved GNGAGG post-repeat sequence. The VK247 repeat consists of a similar organization of the ANGA[G(N/D)]/[DD]QPG motif. The VK247 terminal repeat is consistently comprised of the ANGAGNQPQ motif, which is immediately followed by the conserved ANGAGGQ post-repeat sequence (Rosenberg et al., 1989; Yadava et al., 2007; Zakeri et al., 2006).

Since the sporozoite initiates human infection, the most productive vaccine would block sporozoite invasion of the hepatocyte (Arevalo-Herrera and Herrera, 2001; Billsborough et al., 1997; Herrera et al., 1997, 2005; Yadava et al., 2007). Currently, several *P. vivax* vaccine candidates are in development, targeting proteins such as CSP, merozoite surface protein, duffy binding protein and thrombospondin-related adhesive protein (Arevalo-Herrera and Herrera, 2001; Castellanos et al., 2007; Herrera et al., 1997; Singh et al., 2002, 2005; WHO, 2005; Yadava et al., 2007). Only two *P. vivax* vaccine candidates have been tested in humans (CSP and Pvs25), with an additional few candidates entering into the pre-clinical developmental stage (Herrera et al., 2005, 2007; Malkin et al., 2005). Using the moderately successful vaccine design based on *Plasmodium falciparum* RTS,S (Alonso et al., 2005), several groups have constructed an anti-CSP vaccine for *P. vivax* (Herrera et al., 1997, 2004; WHO, 2005; Yadava et al., 2007). As *P. vivax* vaccine candidates progress toward advanced clinical trials, monitoring the *pvcsp* variant infection status of post-vaccination populations will become an essential aspect of determining the long-term effectiveness of vaccines targeting both PvCSP variants.

In Papua New Guinea (PNG) *P. vivax* causes significant infection and disease. Our studies in northern coastal regions of East Sepik and Madang Provinces over the past ten years have shown that prevalence of malaria has varied with significant reduction in all four species in recent years (Kasehagen et al., 2006; Mehlotra et al., 2000, 2002; Mueller et al., 2009). During this time, minimum PCR-based prevalence of infection by the four human malaria parasite species have been reported as: *P. falciparum*, 30%; *P. vivax*, 25%; *Plasmodium malariae*, 12%; *Plasmodium ovale*, 4%. Minimum infection prevalence determined by less sensitive blood smear light microscopy has always been significantly lower: *P. falciparum*,

20%; *P. vivax*, 9%; *P. malariae*, 1%; *P. ovale*, not detected. Monitoring population level diversity of *P. vivax* will require molecular diagnostic tools and sequence analysis (Cole-Tobian and King, 2003; Cole-Tobian et al., 2002). Here, we analyzed several *pvcsp* representatives in PNG in order to develop a new high-throughput molecular method for assessing prevalence and diversity of VK210 and VK247 variants. Our results provide new insight into *P. vivax* strain diversity in two malaria endemic regions of northern PNG.

2. Materials and methods

2.1. Study areas, populations and blood sample collection

Cross-sectional studies were conducted in two regions of PNG. Twenty-nine villages in the Wosera region located in East Sepik Province and three villages in Mugil located in Madang Province were surveyed as part of collaborative research studies between Case Western Reserve University and PNG Institute of Medical Research (PNGIMR). These two regions of PNG represent distinctly different populations, which are separated by 350 km of rugged terrain. Migration in between locations is not possible by road. Genton et al. (1995) and Mehlotra et al. (2002) have further discussed details about the Wosera and Mugil study sites, respectively.

A total of 703 blood samples were collected from study participants in the Wosera region between August 2001 and June 2003. This sample set, randomly selected from 29 villages (Kasehagen et al., 2006), represented 7.9% of the population (total population ($n = 13,000$)) and included individuals <1–7 years old. A total of 986 blood samples were collected from three villages in the Mugil study site between June and July 1999. This sample set represented 79.4% of the population (total population $n = 1242$) and included individuals <1–85 years old (Cole-Tobian et al., 2002). Demographic information and finger prick blood samples were collected from each study participant. Blood samples were used for thick and thin smears and enable human host and parasite DNA extraction for further diagnostic analysis. Informed consent was obtained from all adult participants and from the parents/legal guardians of minor participants. All protocols were approved by Human Investigations Institutional Review Boards of Case Western Reserve University, University Hospitals Case Medical Center and the Papua New Guinea Medical Research Advisory Committee.

2.2. DNA template preparation

DNA was extracted from whole blood (200 μ L) using the QIAamp 96 DNA Blood Kit (QIAGEN, Valencia, CA).

2.3. Molecular diagnosis of *Plasmodium* species infection

We have previously described strategies and methods to perform PCR and post-PCR ligation detection reaction-fluorescent microsphere assay (LDR-FMA) diagnosis of *Plasmodium* species (McNamara et al., 2006).

2.4. Molecular diagnosis of *P. vivax* CSP variants

For *P. vivax* strain analysis, nested PCR was performed to amplify the *pvcsp* region of the *P. vivax* genome. Previously published sequences for VK210 [GenBank accession no. M11926 (Arnot et al., 1985)] and VK247 [GenBank accession no. M28745 (Rosenberg et al., 1989)] were used to design PCR primers to amplify region I, pre-repeat, central repeated region, and post-repeat conserved region of *pvcsp*, consisting of a fragment 600–750 bp in length (Imwong et al., 2005; Zakeri et al., 2006).

PCR amplification reactions (25 μ l) were performed in buffer containing 3 pmol of appropriate upstream and downstream primers, 67 mM Tris-HCl, pH 8.8, 6.7 mM MgCl₂,

16.6 mM (NH₄)₂SO₄, 10 mM 2-mercaptoethanol, 100 μM dATP, dGTP, dCTP, and dTTP, and 2.5 units of thermostable DNA polymerase using the MJ Research PTC-225 thermocycler (Watertown, MA). The nest-1 primers were Up 5'-ATGTAGATCTGTCCAAGGCCATAAA-3' and Dn 5'-TAATTGAATAATGCTAGGACTAACAATATG-3'; the thermocycling conditions were: 95 °C 2 min (1 ×), 95 °C 30 s, 64 °C 30 s, 72 °C 1 min 30 s (30×), 72 °C 4 min (1×). The nest-2 primers were Up 5'-GCAGAACCACAAAAATCCACGTGAAAATAAG-3' and Dn 5'-CCAACGG-TAGCTCTAACTTTATCTAGGTAT-3'; the thermocycling conditions were: 95 °C 2 min (1 ×), 95 °C 30 s, 64 °C 30 s, 72 °C 1 min 30 s (30×), 72 °C 4 min (1×). To evaluate overall amplification efficiency, PCR products were separated by electrophoresis on 2% agarose gels (1 × TBE), stained with SYBR® Gold (Molecular Probes, Eugene, OR), and visualized on a Storm 860 using ImageQuant, 5.2 software (Molecular Dynamics, Sunnyvale, CA) (Fig. 1).

Following nest-2 PCR amplification, products were subjected to a multiplex ligation detection reaction (LDR) where variant-specific upstream primers ligate to conserved sequence primers when appropriate target sequences are available (Table 1). Previous publications in addition to our DNA sequence results have reported (regardless of the number of repeats within the VK210 and VK247 alleles) that the terminal repeat segment of VK210 ended consistently in a “GDRAAGQPA” amino acid motif; VK247 ended consistently with “ANGAGNQPQ” (Table 2) (Arnot et al., 1985; Rosenberg et al., 1989; Zakeri et al., 2006). Immediately downstream of the repeat, VK210 and VK247 sequences are characterized by conserved amino acid sequences “GNGAGGQAA” and “ANGAGGQAA”, respectively. Based on these observations, Fig. 2 and Table 2 show that repeat-specific LDR primers were designed to hybridize to the VK210 and VK247 terminal repeat sequences with degeneracy introduced to account for reported sequence polymorphisms (Table 2; H = A, C or T; R = G or A; W = A or T; Y = T or C). To the 5' end of both repeat-specific primers, we added unique 24-based FlexMAP™ “TAG” extensions (Luminex Corp., Austin, TX). Conserved sequence primers positioned immediately downstream from the terminal repeat primers were 5' phosphorylated and 3' biotinylated by the supplier (Integrated DNA Technologies, Coralville, IA).

The LDRs were conducted in a solution (15 μL) containing 20 mM Tris-HCl buffer, pH 7.6, 25 mM potassium acetate, 10 mM magnesium acetate, 1 mM MNAD⁺, 10 mM dithiothreitol, 0.1% Triton X-100, 10 nM (200 pmol) of each LDR probe, 1 μL of each PCR product and 2 units of Taq DNA ligase (New England Biolabs, Beverly, MA). Reactions were initially heated at 95 °C for 1 min, followed by 32 thermal cycles at 95 °C for 15 s (denaturation) and 58 °C for 2 min (annealing/ligation).

The 5' end of the LDR products received classification labeling in a second multiplex reaction where hybridization occurs between anti-TAG oligonucleotide probes bound to fluorescent micro-spheres and the TAG sequences added to the *pvcsp* strain repeat-specific primers. The multiplex LDR product (5 μL) was added to 60 μL of hybridization solution (3 M tetramethylammonium chloride [TMAC], 50 mM Tris-HCl, pH 8.0, 3 mM EDTA, pH 8.0, 0.10% sodium dodecyl sulfate) containing 250 beads from specific Luminex® FlexMAP™ microsphere sets. Mixtures were heated to 95 °C for 90 s and incubated at 37 °C for 40 min to allow hybridization between species-specific LDR products and bead-labeled anti-TAG probes in Costar-6511 M polycarbonate 96-well V-bottom plates (Corning Inc., Corning, NY).

After hybridization, reaction products were incubated in a solution containing streptavidin-R-phycoerythrin (Invitrogen, Carlsbad, CA) to allow reporter labeling through binding to the 3'-biotin on the conserved sequence primers. Hybridized product (65 μL) was added to a

solution containing streptavidin-R-phycoerythrin (6 μL) in TMAC hybridization solution (20 $\text{ng}/\mu\text{L}$) and incubated at 37 $^{\circ}\text{C}$ for 40 min.

Detection of doubly labeled ligation products was performed using a Bio-Plex array reader (Bio-Rad Laboratories, Hercules, CA); plate temperatures were set to 37 $^{\circ}\text{C}$ throughout detection. This instrument was optimized to excite red/infra-red classification fluorochromes in embedded microspheres (proprietary Luminex technology). Further details are provided in McNamara et al. (2006). Differentiation of positive fluorescent signals was determined using the median fluorescence intensity plus three times the standard deviation of the whole sample data set. For both VK210 (microsphere 28) and VK247 (microsphere 80), the accepted positive value for fluorescence was approximately 500, thus any fluorescent signals above this value was considered positive for the corresponding *P. vivax* strains.

2.5. DNA sequence analysis

Direct DNA sequence analysis for select samples ($n = 18$) from both the Wosera and Mugil regions was performed by dideoxy chain-termination utilizing BigDye version 3.1 (Applied Biosystems) (Quicklane Sequencing, Agencourt Bioscience Corp., Beverly, MA) for the *pvcsp* gene. DNA and amino acid sequence was analyzed using Sequencer 4.6 (GeneCodes Corp., Ann Arbor, MI); sequences analyzed in this study correspond to GenBank accession nos. EU031819–EU031836 (Fig. 3).

2.6. Statistical analysis

Statistical analysis and graphing features were carried out using Graph Pad Prism 4.02 (San Diego, CA) and Microsoft Excel 2007 (Redmond, WA). The multiple-kind lottery (MKL) model was used to calculate the expected numbers of *P. vivax* strain infection assemblages in each population. This model assumes that acquisition of infection by individual parasite strains are independent events, and one possible outcome of exposure is no acquisition of infection. Infection is designated as p_1 , and the reciprocal, absence of infection, is designated as $1-p_1$ or q_1 (Janovy et al., 1995; Mehlotra et al., 2002). Extending this to the two *P. vivax* strains, p_1 and p_2 would represent infection by the individual strains, VK210 and VK247, whereas q_1 and q_2 would represent absence of infection by the individual variants. The expected frequency of infection by one strain alone (e.g., VK210 only) is the product p_1q_2 . Mixed infection by two strains (e.g., VK210 and VK247) is the product p_1p_2 . Chi-square values were calculated using heterogeneity tests (3 degrees of freedom) to compare observed with expected values.

3. Results

3.1. *pvcsp* PCR and sequence analysis

Due to the gene's variable number of repeats, nested PCRs for the *pvcsp* gene produced bands with sizes ranging from 600–750 bp in positive samples; a number of samples with multiple bands per lane were also observed (Fig. 1). After PCR amplification, DNA sequence analysis was performed on 18 samples that showed clear presence of only one *pvcsp* length variant. Our sequence data confirmed previous descriptions of the VK210 and VK247 sequences (Arnot et al., 1985; Rosenberg et al., 1989; Zakeri et al., 2006). The results from our DNA analysis of these 18 sequences (10 Wosera samples [8, VK210; 2, VK247] and 8 Mugil samples [4, VK210; 4, VK247]) (Fig. 3) demonstrated that the terminal repeat (Motif 'B1', GDRAAGQPA) and 27 bp downstream post-repeat region of VK210 sequence was conserved among all VK210 samples, consistent with those previously published (Table 2) (Arnot et al., 1985; Rosenberg et al., 1989; Zakeri et al., 2006). Similarly, the terminal repeat (Motif 'D2', ANGAGNQPQ) and 27 bp of the post-repeat region of VK247 sequences was conserved among all VK247 samples, consistent

with previously published VK247 sequences and different from VK210 sequences (Table 2) (Rosenberg et al., 1989; Zakeri et al., 2006). These observations allowed for the development of our *pvcsp* LDR-FMA diagnostic assay (Fig. 2, Tables 1 and 2).

In addition to characterizing the terminal repeat regions of the *pvcsp* gene, we observed significant diversity within the repeated region. Fig. 3 demonstrates that *pvcsp* repeat regions ranged in size from 17 to 20 repeats as shown by blocks representing the various 9-amino acid sequence motifs. The predominant sequence motifs for VK210 were GDRADGQPA (Motif 'A') and GDRAAGQPA (Motif 'B') and for VK247, ANGAGNQPG (Motif 'D') and ANGAGDQPG (Motif 'E'). Due to the relatively small number of samples sequenced, the VK210 minority repeat Motif 'C' (GDRAPGQPA) was not observed, whereas the VK247 minority repeat Motif 'F' (ANGADDQPG) was observed in four samples sequenced. We also found that no two *pvcsp* sequences were alike at the nucleotide level as indicated in the alpha-numeric codes assigned to the specific repeat units (Fig. 3). Additionally, synonymous nucleotide sequence differences were observed within each repeat motif; those with the same 'Motif Letter' and 'Number' combination share the exact same nucleotide sequence. Overall, we observed eight different variants of the amino acid 'A' motif (A1–A8), six variants of the 'B' motif (B1–B6), six variants of the 'D' motif (D1–D6), three variants of the 'E' motif (E1–E3) and three variants of the 'F' motif (F1–F3).

3.2. Application and evaluation of the *pvcsp* LDR-FMA

Based on the sequence analysis, we designed sequence-specific LDR-FMA to diagnose infection by different *P. vivax* strains. We applied this diagnostic assay in a survey of samples from two different malaria-endemic regions of northern PNG, the Wosera ($n = 703$) and Mugil ($n = 986$). This analysis included the 18 samples evaluated by DNA sequence analysis. Results showed 100% concordance between the LDR-FMA strain assessment and DNA sequence analysis for the 18 samples described in Fig. 3. Overall evaluation of individual infections showed that 14.2% ($n = 239$) of study participants were infected with VK210 alone, 5.2% ($n = 88$) infected with VK247 alone, 10.7% ($n = 180$) samples were characterized as a mixed infection with both strains, and 1182 samples were classified as not infected with either VK210 or VK247. Fifteen samples from the Wosera (coded as DFA-DFD) and 15 samples from the Mugil (coded as VFA) study sites were chosen to provide an overview of the VK210 and VK247-strain-specific fluorescence generated by the *pvcsp* LDR-FMA (Fig. 4). These results show that the infections are characterized by a wide range of fluorescent signals for the two strains. The data also shows that some infections with both strains were dominated by VK210 (fluorescence VK210 > VK247), while other mixed infections were dominated by VK247 (fluorescence VK247 > VK210); some infections show relatively similar fluorescence for both VK210 and VK247.

Because all of the Wosera and Mugil samples have been previously evaluated for *Plasmodium* infections by a species-specific LDR-FMA diagnostic assay (McNamara et al., 2006), we compared *pvcsp* repeat-positivity with *P. vivax* infection status (Cole-Tobian et al., 2002; Kasehagen et al., 2006). *Plasmodium* species-specific LDR-FMA analysis of the two sample sets ($n = 1689$) indicated that 507 samples were infected with *P. vivax*: 199 from the Wosera, 308 from Mugil. By the *pvcsp* LDR-FMA analysis, 228 individuals from the Wosera and 279 individuals from Mugil were found to be infected with *P. vivax*. Overall, concordance between the detection of *P. vivax* by the *Plasmodium* species and *pvcsp* assays was 87% in the Wosera and 81% in Mugil (Table 3a and b).

3.3. Distribution of infection with VK210 and VK247 strains

We further compared our findings between Wosera and Mugil to determine if there were differences in the prevalence and distribution of the VK210 and VK247 strains in different regions of northern PNG. Although our results (Table 4) suggested that among infected people the VK210 strain was more predominant in Mugil (240/279; 86.0%) than in the Wosera (179/228; 78.5%), there was no significant difference in the distribution of VK210 and VK247 between these two different study sites (χ^2 p -value = 0.068).

Finally, we wanted to evaluate how the VK210 and VK247 strains were distributed within a vivax-endemic community. Our null hypothesis was that the *pvcsp* strains would be randomly distributed. The multiple-kind lottery model (MKL; assumes random distribution) (Janovy et al., 1995) was used to calculate the expected frequencies of all combinations of the VK210 and VK247 strains (VK210 alone, VK247 alone, VK210 + VK247, and no infection). Results for both study sites showed that there was a significant difference in the distribution of observed and expected infections (Wosera: $\chi^2 = 122.12$, $p > 0.001$, 3 degrees of freedom; Mugil: $\chi^2 = 197.68$, $p > 0.001$, 3 degrees of freedom). Fig. 5a and b illustrates that the observed frequencies of single-strain infections were lower, and the observed frequencies of the VK210 + VK247 mixed infections were at least 2-fold higher than expected.

4. Discussion

Frequencies of the predominant *P. vivax* circumsporozoite protein variants (VK210 and VK247) have been determined in a number of malaria-endemic countries around the world, motivated by potential that parasite populations may respond differently to PvCSP-based vaccines. While Kain et al. (1992) analyzed 10 *P. vivax*-positive samples from PNG reporting 3 VK247, 6 mixed, and 1 VK210 allele, it is not possible to assess *pvcsp* strain frequencies based on this limited set of samples. By analyzing a large sample set from different study sites, we designed our study to provide a more widespread assessment of *pvcsp* strain diversity in *P. vivax*-endemic regions of northern PNG. For this, we developed a new assay to analyze the distribution of the *P. vivax* VK210 and VK247 strains, based on sequence differences in the repeated region of *pvcsp*, in a high-throughput 96-well format. Preliminary results showed 100% concordance between DNA sequence and LDR-FMA analysis. We then applied this assay to samples from two distinct *P. vivax*-endemic areas in PNG, the Wosera (East Sepik Province) and Mugil (Madang Province). Single-strain infections with VK210 predominated in both study sites (Wosera 42%, Mugil 52%) followed by mixed-strain infections (Wosera 37%, Mugil 34%). Single-strain infections with VK247 were least prevalent (Wosera 21%, Mugil 14%).

A growing number of molecular diagnostic surveys have reported VK210 and VK247 strain prevalence data from regions of the world where *P. vivax* transmission occurs (Bonilla et al., 2006; Cui et al., 2003; Imwong et al., 2005; Kain et al., 1993b; Kim et al., 2006; Leclerc et al., 2004; Machado and Póvoa, 2000; Moon et al., 2009; Silva et al., 2006; Storti-Melo et al., 2009; Zakeri et al., 2006, 2009, 2010). Table 5 presents a summary of the *pvcsp* strain frequencies from infected individuals. This overview shows that VK210 is the predominant *pvcsp* strain observed throughout the world, and suggests that frequencies of the VK247 strain is distributed heterogeneously with the highest prevalence of this strain reported to date occurring in Thailand (Kain et al., 1993a) and PNG (this study). Within Thailand one earlier study found that VK247 was the predominant *P. vivax* strain among study participants from the Royal Thai Army (Kain et al., 1992). Additionally, while VK210 was the predominant *pvcsp* variant detected among *Anopheles* mosquitoes collected during 1986–87 in Madang Province, an IgG-based serological survey of the human population in this region revealed more frequent infections with the VK247 than with the VK210 variant

(Burkot et al., 1992). With further consideration of these two *pvcsp* variants, there appears to be evidence that VK247 may have been the predominant strain in multiple locations in the Asian region. Although difficult to confirm, the combined data suggest that a shift from predominance of VK247 to VK210 may have occurred in some regions. Differences in the distribution pattern of VK210 and VK247 strains may be important to consider as PvCSP is included in current *P. vivax* vaccine strategies.

On closer examination of our prevalence data we found that the number of mixed-strain infections significantly exceeded their expected prevalence. In both Mugil and Wosera we observed 2.5 times more mixed-strain infections than expected. As described earlier the hypnozoite, the dormant liver stage of the *P. vivax* lifecycle, can be reactivated months after initial infection (Krotoski et al., 1986). We hypothesize that a greater than expected number of mixed-strain infections in our PNG study may reflect cumulative exposure through new infections and reactivated hypnozoites.

A recent study from the Acre State of Western Brazil described a new motif (GNGAGGQAA) in the VK210 sequence, as well as polymorphism which suggests that VK210 may not always end in the 'B1' (GDRAAGQPA) terminal repeat (Patil et al., 2010). While the discordance observed between our *P. vivax* species diagnostic assay and the *pvcsp* assay (*P. vivax*+/*pvcsp*-) suggests that there may be terminal repeats other than the 'B1' sequence, we were not able to perform DNA sequence analysis because these samples did not support PCR amplification of the *pvcsp* fragment. This suggested that there may be polymorphism flanking the *pvcsp* repeat in PCR primer annealing sites. Potential polymorphism can be identified in advance by DNA sequence analysis, and revised strategies needed for different regional surveys can be easily developed using our LDR-FMA assay.

Molecular diagnostic assays will be essential tools for monitoring parasite populations throughout the world as various interventions are implemented. The LDR-FMA described here improves efficiency of molecular diagnosis by reducing manipulations, as all steps of the procedure are handled in 96-well format and the assay data is deposited from the detection instrument directly into standard spreadsheet format. As polymorphisms categorizing *P. vivax* strains are identified through fluorescent signals, discrimination between uninfected and infected (VK201 alone, VK247 alone or VK210 + VK247 mixed) samples is easily performed through uniform objective methods; subjective interpretation of presence or absence of RFLP bands and low-resolution of RFLP band size is eliminated by this assay. While the current assay has not been developed to assess *pvcsp* diversity beyond VK210 and VK247 strains, the multiplex method can be expanded through addition of probes to identify other strain-specific marker sequence. Our data, compiled with what is known about *P. vivax* infections in other malaria-endemic regions of the world, would suggest that strain diversity will challenge *P. vivax* control and elimination.

Acknowledgments

We would like to thank the study participants of both the Wosera and Mugil study areas for their participation. We thank Lauren J. Kasehagen, Ph.D., and Jennifer Cole-Tobian, Ph.D., for assistance with analysis and database organization and Benson Kiniboro and Moses Baisor for coordinating the collection of field samples used in this study. We also thank Rajeev Mehlotra for his helpful comments during manuscript preparation. Financial support: This study was supported by a grant from the Fogarty International Center of the National Institutes of Health (NIH) TW007872.

References

Alonso PL, Sacarlal J, Aponte JJ, Leach A, Macete E, Aide P, Sigauque B, Milman J, Mandomando I, Bassat Q. Duration of protection with RTS, S/ AS02A malaria vaccine in prevention of Plasmodium

- falciparum disease in Mozambican children: single-blind extended follow-up of a randomised controlled trial. *Lancet*. 2005; 366:2012–2018. [PubMed: 16338450]
- Arevalo-Herrera M, Herrera S. *Plasmodium vivax* malaria vaccine development. *Mol. Immunol*. 2001; 38:443–455. [PubMed: 11741694]
- Arnot, DE.; Barnwell, JW.; Tam, JP.; Nussenzweig, V.; Nussenzweig, RS.; Enea, V. *Science*. Vol. 230. New York, N.Y.: 1985. Circumsporozoite protein of *Plasmodium vivax*: gene cloning and characterization of the immunodominant epitope; p. 815-818.
- Bilsborough J, Baumgart K, Bathurst I, Barr P, Good MF. Fine epitope specificity of antibodies to region II of the *Plasmodium vivax* circumsporozoite protein correlates with ability to bind recombinant protein and sporozoites. *Acta Trop*. 1997; 65:59–80. [PubMed: 9164601]
- Bonilla JA, Validum L, Cummings R, Palmer CJ. Genetic diversity of *Plasmodium vivax* Pvcsp and PvmSP1 in Guyana, South America. *Am. J. Trop. Med. Hyg*. 2006; 75:830–835. [PubMed: 17123973]
- Burkot TR, Wirtz RA, Paru R, Garner P, Alpers MP. The population dynamics in mosquitoes and humans of two *Plasmodium vivax* polymorphs distinguished by different circumsporozoite protein repeat regions. *Am. J. Trop. Med. Hyg*. 1992; 47:778. [PubMed: 1471735]
- Carter R, Mendis KN. Evolutionary and historical aspects of the burden of malaria. *Clin. Microbiol. Rev*. 2002; 15:564. [PubMed: 12364370]
- Castellanos A, Arevalo-Herrera M, Restrepo N, Gulloso L, Corradin G, Herrera S. *Plasmodium vivax* thrombospondin related adhesion protein: immunogenicity and protective efficacy in rodents and Aotus monkeys. *Mem. Inst. Oswaldo. Cruz*. 2007; 102:411–416. [PubMed: 17568948]
- Cole-Tobian J, King CL. Diversity and natural selection in *Plasmodium vivax* Duffy binding protein gene. *Mol. Biochem. Parasitol*. 2003; 127:121–132. [PubMed: 12672521]
- Cole-Tobian JL, Cortes A, Baisor M, Kastens W, Xainli J, Bockarie M, Adams JH, King CL. Age-acquired immunity to a *Plasmodium vivax* invasion ligand, the Duffy binding protein. *J. Infect. Dis*. 2002; 186:531–539. [PubMed: 12195381]
- Cui L, Mascorro CN, Fan Q, Rzomp KA, Khuntirat B, Zhou G, Chen H, Yan G, Sattabongkot J. Genetic diversity and multiple infections of *Plasmodium vivax* malaria in Western Thailand. *Am. J. Trop. Med. Hyg*. 2003; 68:613–619. [PubMed: 12812356]
- Genton B, Al-Yaman F, Beck HP, Hii J, Mellor S, Narara A, Gibson N, Smith T, Alpers MP. The epidemiology of malaria in the Wosera area, East Sepik Province, Papua New Guinea, in preparation for vaccine trials. I. Malariometric indices and immunity. *Ann. Trop. Med. Parasitol*. 1995; 89:359. [PubMed: 7487223]
- Guerra CA, Howes RE, Patil AP, Gething PW, Van Boeckel TP, Temperley WH, Kabaria CW, Tatem AJ, Manh BH, Elyazar IR, Baird JK, Snow RW, Hay SI. The international limits and population at risk of *Plasmodium vivax* transmission in 2009. *PLoS. Negl. Trop. Dis*. 2010; 4:e774. [PubMed: 20689816]
- Guerra CA, Snow RW, Hay SI. Mapping the global extent of malaria in 2005. *Trends Parasitol*. 2006; 22:353–358. [PubMed: 16798089]
- Herrera S, Bonelo A, Perlaza BL, Fernandez OL, Victoria L, Lenis AM, Soto L, Hurtado H, Acuna LM, Velez JD, Palacios R, Chen-Mok M, Corradin G, Arevalo-Herrera M. Safety and elicitation of humoral and cellular responses in colombian malaria-naive volunteers by a *Plasmodium vivax* circum-sporozoite protein-derived synthetic vaccine. *Am. J. Trop. Med. Hyg*. 2005; 73:3–9. [PubMed: 16291760]
- Herrera S, Bonelo A, Perlaza BL, Valencia AZ, Cifuentes C, Hurtado S, Quintero G, Lopez JA, Corradin G, Arevalo-Herrera M. Use of long synthetic peptides to study the antigenicity and immunogenicity of the *Plasmodium vivax* circumsporozoite protein. *Int. J. Parasitol*. 2004; 34:1535–1546. [PubMed: 15582530]
- Herrera S, Corradin G, Arevalo-Herrera M. An update on the search for a *Plasmodium vivax* vaccine. *Trends Parasitol*. 2007; 23:122–128. [PubMed: 17258937]
- Herrera S, De Plata C, Gonzalez M, Perlaza BL, Bettens F, Corradin G, Arevalo-Herrera M. Antigenicity and immunogenicity of multiple antigen peptides (MAP) containing *P. vivax* CS epitopes in Aotus monkeys. *Parasite Immunol*. 1997; 19:161–170. [PubMed: 9149283]

- Imwong M, Pukrittayakamee S, Grüner AC, Rénia L, Letourneur F, Looareesuwan S, White NJ, Snounou G. Practical PCR genotyping protocols for *Plasmodium vivax* using PvcS and PvmSp1. *Malar. J.* 2005; 4:20. [PubMed: 15854233]
- Janovy J Jr, Clopton RE, Clopton DA, Snyder SD, Efting A, Krebs L. Species density distributions as null models for ecologically significant interactions of parasite species in an assemblage. *Ecol. Model.* 1995; 77:189–196.
- Kain KC, Brown AE, Lanar DE, Ballou WR, Webster HK. Response of *Plasmodium vivax* variants to chloroquine as determined by microscopy and quantitative polymerase chain reaction. *Am. J. Trop. Med. Hyg.* 1993a; 49:478. [PubMed: 8214278]
- Kain KC, Brown AE, Mirabelli L, Webster HK. Detection of *Plasmodium vivax* by polymerase chain reaction in a field study. *J. Infect. Dis.* 1993b; 168:1323–1326. [PubMed: 8228373]
- Kain KC, Brown AE, Webster HK, Wirtz RA, Keystone JS, Rodriguez MH, Kinahan J, Rowland M, Lanar DE. Circumsporozoite genotyping of global isolates of *Plasmodium vivax* from dried blood specimens. *J. Clin. Microbiol.* 1992; 30:1863–1866. [PubMed: 1629344]
- Kasehagen LJ, Mueller I, McNamara DT, Bockarie MJ, Kiniboro B, Rare L, Lorry K, Kastens W, Reeder JC, Kazura JW. Changing patterns of *Plasmodium* blood-stage infections in the wosera region of Papua New Guinea monitored by light microscopy and high throughput PCR diagnosis. *Am. J. Trop. Med. Hyg.* 2006; 75:588–596. [PubMed: 17038678]
- Kim JR, Imwong M, Nandy A, Chotivanich K, Nontprasert A, Tonomsing N, Maji A, Addy M, Day NPJ, White NJ. Genetic diversity of *Plasmodium vivax* in Kolkata, India. *Malar. J.* 2006; 5:71. [PubMed: 16907979]
- Krotoski WA, Garnham PCC, Cogswell FB, Collins WE, Bray RS, Gwadz RW, Killick-Kendrick R, Wolf RH, Sinden R, Hollingdale M. Observations on early and late post-sporozoite tissue stages in primate malaria. IV. Preerythrocytic schizonts and/or hypnozoites of Chesson and North Korean strains of *Plasmodium vivax* in the chimpanzee. *Am. J. Trop. Med. Hyg.* 1986; 35:263. [PubMed: 3513645]
- Leclerc MC, Menegon M, Cligny A, Noyer JL, Mammadov S, Aliyev N, Gasimov E, Majori G, Severini C. Genetic diversity of *Plasmodium vivax* isolates from Azerbaijan. *Malar. J.* 2004; 3:40. [PubMed: 15535878]
- Machado RLD, Póvoa MM. Distribution of *Plasmodium vivax* variants (VK210, VK247 and *P. vivax*-like) in three endemic areas of the Amazon region of Brazil and their correlation with chloroquine treatment. *Trans. R. Soc. Trop. Med. Hyg.* 2000; 94:377–381. [PubMed: 11127238]
- Malkin EM, Durbin AP, Diemert DJ, Sattabongkot J, Wu Y, Miura K, Long CA, Lambert L, Miles AP, Wang J, Stowers A, Miller LH, Saul A. Phase 1 vaccine trial of Pvs25H: a transmission blocking vaccine for *Plasmodium vivax* malaria. *Vaccine.* 2005; 23:3131–3138. [PubMed: 15837212]
- McNamara DT, Kasehagen LJ, Grimberg BT, Cole-Tobian J, Collins WE, Zimmerman PA. Diagnosing infection levels of four human malaria parasite species by a polymerase chain reaction/ligase detection reaction fluorescent microsphere-based assay. *Am. J. Trop. Med. Hyg.* 2006; 74:413–421. [PubMed: 16525099]
- Mehlotra RK, Kasehagen LJ, Baisor M, Lorry K, Kazura JW, Bockarie MJ, Zimmerman PA. Malaria infections are randomly distributed in diverse holoendemic areas of Papua New Guinea. *Am. J. Trop. Med. Hyg.* 2002; 67:555–562. [PubMed: 12518843]
- Mehlotra RK, Lorry K, Kastens W, Miller SM, Alpers MP, Bockarie M, Kazura JW, Zimmerman PA. Random distribution of mixed species malaria infections in Papua New Guinea. *Am. J. Trop. Med. Hyg.* 2000; 62:225–231. [PubMed: 10813477]
- Mendis K, Sina BJ, Marchesini P, Carter R. The neglected burden of *Plasmodium vivax* malaria. *Am. J. Trop. Med. Hyg.* 2001; 64:97–106. [PubMed: 11425182]
- Moon SU, Lee HW, Kim JY, Na BK, Cho SH, Lin K, Sohn WM, Kim TS. High frequency of genetic diversity of *Plasmodium vivax* field isolates in Myanmar. *Acta Trop.* 2009; 109:30–36. [PubMed: 18851938]
- Mueller I, Widmer S, Michel D, Maraga S, McNamara DT, Kiniboro B, Sie A, Smith TA, Zimmerman PA. High sensitivity detection of Plasmodium species reveals positive correlations between

- infections of different species, shifts in age distribution and reduced local variation in Papua New Guinea. *Malar. J.* 2009; 8:41. [PubMed: 19284594]
- Patil A, Orjuela-Sanchez P, da Silva-Nunes M, Ferreira M. Evolutionary dynamics of the immunodominant repeats of the *Plasmodium vivax* malaria-vaccine candidate circumsporozoite protein (CSP). *Infect. Genet. Evol.* 2010; 10:298–303. [PubMed: 20097310]
- Rosenberg, R.; Wirtz, RA.; Lanar, DE.; Sattabongkot, J.; Hall, T.; Waters, AP.; Prasittisuk, C. *Science*. Vol. 245. New York, N.Y.: 1989. Circumsporozoite protein heterogeneity in the human malaria parasite *Plasmodium vivax*; p. 973-976.
- Silva ANM, Santos CCB, Lacerda RN, Machado RLD, Póvoa MM. Susceptibility of *Anopheles aquasalis* and *An. darlingi* to *Plasmodium vivax* VK210 and VK247. *Mem. Inst. Oswaldo Cruz.* 2006; 101:547–550. [PubMed: 17072460]
- Singh AP, Ozwara H, Kocken CHM, Puri SK, Thomas AW, Chitnis CE. Targeted deletion of *Plasmodium knowlesi* duffy binding protein confirms its role in junction formation during invasion. *Mol. Microbiol.* 2005; 55:1925–1934. [PubMed: 15752210]
- Singh AP, Puri SK, Chitnis CE. Antibodies raised against receptor-binding domain of *Plasmodium knowlesi* duffy binding protein inhibit erythrocyte invasion. *Mol. Biochem. Parasitol.* 2002; 121:21–31. [PubMed: 11985860]
- Storti-Melo LM, de Souza-Neiras WC, Cassiano GC, Joazeiro ACP, Fontes CJ, Bonini-Domingos CR, D'Almeida Couto Á, Povoia MM, de Mattos LC, Cavasini CE. *Plasmodium vivax* circumsporozoite variants and duffy blood group genotypes in the Brazilian Amazon region. *Trans. R. Soc. Trop. Med. Hyg.* 2009; 103:672–678. [PubMed: 18804827]
- WHO. Portfolio of Candidate Malaria Vaccines Currently in Development March 2005. WHO; 2005.
- Yadava A, Sattabongkot J, Washington MA, Ware LA, Majam V, Zheng H, Kumar S, Ockenhouse CF. A novel chimeric *Plasmodium vivax* circumsporozoite protein induces biologically functional antibodies that recognize both VK210 and VK247 sporozoites. *Infect. Immun.* 2007; 75:1177–1185. [PubMed: 17158893]
- Zakeri S, Abouie Mehrizi A, Djadid ND, Snounou G. Circumsporozoite protein gene diversity among temperate and tropical *Plasmodium vivax* isolates from Iran. *Trop. Med. Int. Health.* 2006; 11:729–737. [PubMed: 16640626]
- Zakeri S, Raeisi A, Afshar M, Kakar Q, Ghasemi F, Atta H, Zamani G, Memon MS, Salehi M, Djadid ND. Molecular characterization of *Plasmodium vivax* clinical isolates in Pakistan and Iran using pvmsp-1, pvmsp-3alpha and pvmsp genes as molecular markers. *Parasitol. Int.* 2009
- Zakeri S, Safi N, Afshar M, Butt W, Ghasemi F, Mehrizi AA, Atta H, Zamani G, Djadid ND. Genetic structure of *Plasmodium vivax* isolates from two malaria endemic areas in Afghanistan. *Acta Trop.* 2010; 113:12–19. [PubMed: 19716798]

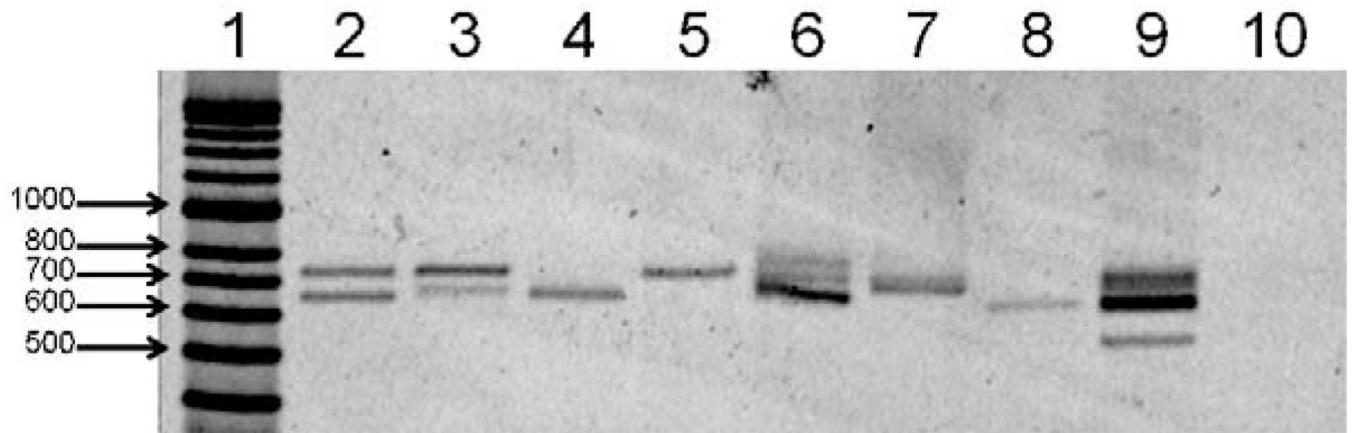


Fig. 1. Representative *pvcsp* Nest-2 PCR products on 2% agarose gel. Lane 1: HyperLadder II (Bioline USA Inc., Taunton, MA). Lanes 2–5: representative samples from Wosera, lanes 6–9: representatives from Mugil. Lane 10: blank, negative control. Samples in lanes 2–4, 6 and 9 were judged ‘mixed’ infections according to the *pvcsp* LDR-FMA. Lanes 5 and 7 were positive for single VK247 infection and lane 8 was positive for single VK210 by *pvcsp* LDR-FMA.

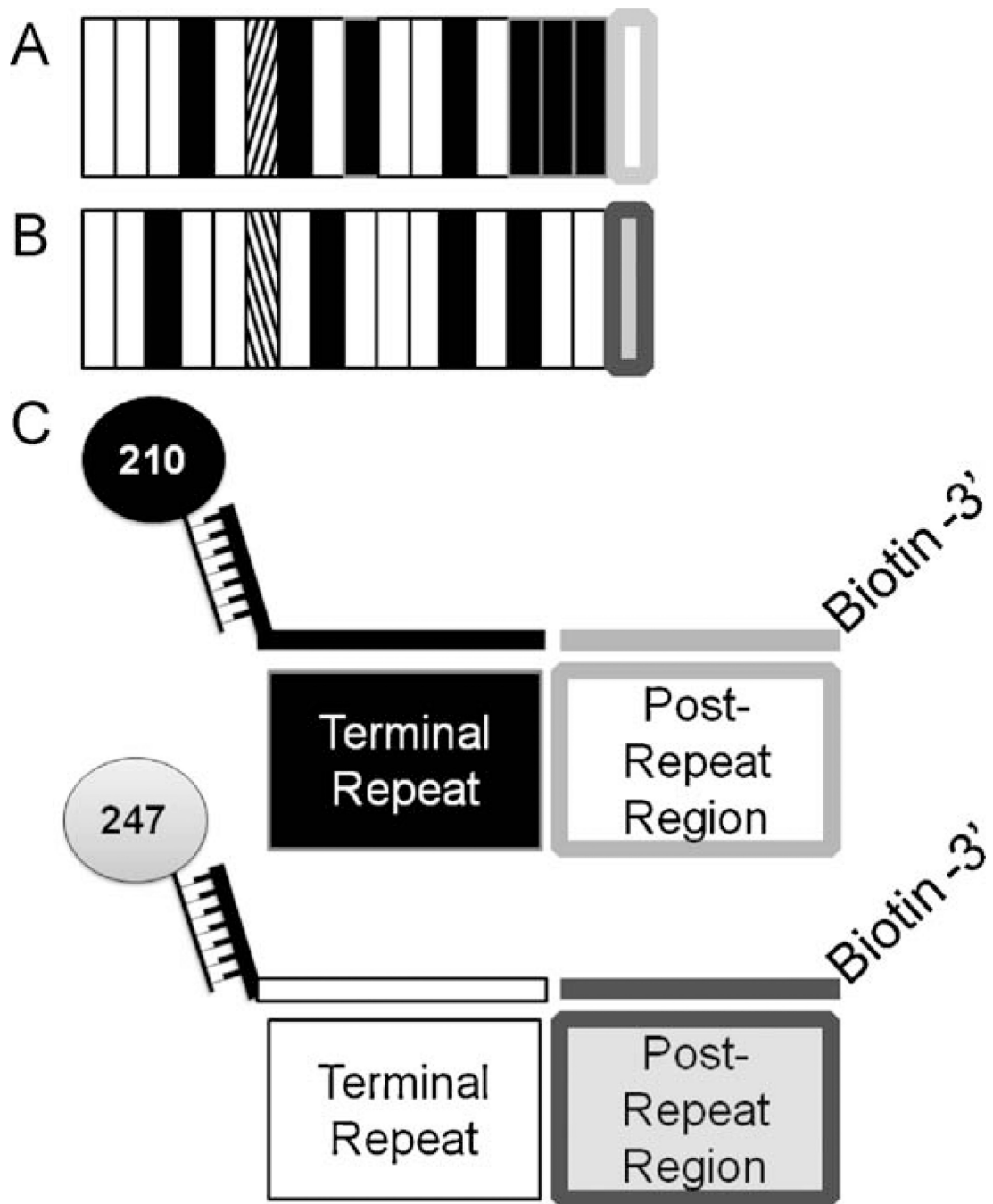


Fig. 2. Post-PCR ligation detection reaction-fluorescent microsphere assay (LDR-FMA) design. *Plasmodium species* and *pvcsp* strain infection were analyzed using post-PCR LDR-FMA. Species diagnosis was performed as previously described in McNamara et al. (2006). *P. vivax* strain diagnosis based on variants VK210 and VK247 were performed as shown here. (A) VK210 *pvcsp* repeat region genetic structure. White bars represent ‘A’ repeat motifs, black bars – ‘B’ repeat motifs, and diagonal bars – ‘C’ repeat motif. The conserved post-repeat region is shown as a white box outlined in light grey. These A, B, and C motifs as well as post-repeat sequences are unique to VK210. (B) VK247 *pvcsp* repeat region genetic structure. White bars represent ‘D’ repeat motifs, black bars – ‘E’ repeat motifs, and

diagonal bars – ‘F’ repeat motifs. The light grey box outlined in dark grey represents the conserved post-repeat region. These D, E, and F motifs as well as post-repeat sequences are unique to VK247. (C) Illustrates the LDR primer design capturing the terminal repeat and post-repeat region unique to each *P. vivax* strain.

VK 210 Amino Acid Alignment

| | | | | | | | | | | | | | | | | | | | |
|--------|---------|----|----|----|----|----|----|----|----|----|----|----|----|----|----|----|----|----|----|
| Wosera | DFB2526 | A1 | B2 | A1 | A1 | A1 | B2 | A1 | A1 | B1 | A1 | B3 | B1 | A5 | B1 | A6 | B1 | B1 | |
| | DFD579 | A1 | A1 | A1 | B2 | A1 | B5 | A2 | B1 | A2 | B1 | A2 | B3 | B2 | A3 | B1 | A3 | B1 | |
| | DFC234 | A1 | A4 | A4 | B2 | A1 | B5 | A2 | B1 | A2 | B3 | B2 | A1 | B4 | A6 | B1 | B1 | B1 | |
| | DFC300 | A1 | A4 | A4 | B3 | A1 | B5 | A1 | B1 | A2 | B3 | B2 | A1 | B4 | A6 | B1 | B1 | B1 | |
| | DFC1908 | A1 | A1 | A1 | B2 | A1 | A1 | B1 | A2 | B1 | B1 | A2 | B3 | B2 | A3 | B1 | A4 | B1 | B1 |
| | DFC2390 | A8 | A4 | A4 | B2 | A1 | B6 | A2 | B1 | A2 | A7 | A2 | B3 | B2 | A3 | B1 | A7 | B1 | B1 |
| | DFD191 | A8 | A4 | A4 | B2 | A1 | B5 | A2 | B1 | A2 | A7 | A2 | B3 | B2 | A3 | B1 | A3 | B1 | B1 |
| | DFB329 | A1 | A1 | A5 | B2 | A5 | B6 | A5 | B1 | A2 | B3 | B2 | A1 | B5 | A1 | B1 | B1 | B1 | |
| Mugil | VFA 414 | A1 | A1 | A1 | B2 | A1 | B4 | A2 | B1 | A2 | B3 | B2 | A1 | B4 | A6 | B1 | B1 | B1 | |
| | VFA 21 | A1 | A1 | A1 | B2 | A1 | B6 | A1 | B1 | A2 | B3 | B2 | A1 | B4 | A6 | B1 | B1 | B1 | |
| | VFA 200 | A1 | A1 | A1 | B2 | A1 | B4 | A1 | B1 | A2 | B3 | B2 | A1 | B4 | A1 | B1 | B1 | B1 | |
| | VFA 215 | A1 | A1 | A1 | B2 | A1 | B6 | A1 | B1 | A2 | B1 | A2 | B3 | B2 | A3 | B1 | A3 | B1 | B1 |

A GDRADGQPA
B GDRAAGQPA

VK 247 Amino Acid Alignment

| | | | | | | | | | | | | | | | | | | | | | |
|--------|---------|----|----|----|----|----|----|----|----|----|----|----|----|----|----|----|----|----|----|----|----|
| Wosera | DFB3032 | D3 | D3 | E1 | D1 | E1 | D1 | D1 | D1 | F1 | D3 | D1 | D2 | E1 | D1 | E1 | D4 | D2 | D1 | D2 | |
| | DFC1921 | D3 | D3 | D3 | D3 | D1 | D1 | D1 | D1 | F1 | D3 | D1 | E2 | E1 | D1 | E1 | D4 | D3 | D1 | D2 | |
| | VFA 461 | D3 | D1 | D1 | D3 | D3 | D1 | D2 | E2 | D1 | D2 | E1 | D1 | E1 | D4 | D2 | D1 | D2 | | | |
| | VFA 269 | D3 | D3 | D1 | D1 | D1 | F2 | D5 | D1 | D2 | E1 | D1 | D2 | E1 | D1 | E1 | D4 | D2 | D1 | D2 | |
| | VFA 514 | E3 | D5 | D3 | D3 | D1 | D1 | D6 | D3 | D1 | D2 | D2 | D1 | D2 | E1 | D1 | E1 | D1 | D2 | D1 | D2 |
| | VFA 530 | E1 | D1 | D3 | F3 | D3 | D1 | D2 | E1 | D1 | E1 | D1 | D2 | D1 | E1 | D4 | D2 | D1 | D2 | | |

D ANGAGNQPG
E ANGAGDQPG
F ANGADDQPG

Fig. 3.

DNA sequence analysis of eighteen PNG samples. VK210 (top) and VK247 (bottom) were analyzed from both Wosera and Mugil. Sample ID codes correspond to individual isolates. Repeats are classified using uniquely shaded blocks; each block corresponds to a different amino acid repeat motif observed in the sequenced sample (VK210 motifs A–C; VK247 D–F). Samples were found to exhibit 17–20 repeats. Two of the three recognized repeated sequence motifs (A and B) were observed with VK210 isolates. The minor VK210 motif, motif C (GDRAPGQPA) was not observed in any of our samples. We observed all three VK247 repeat sequence motifs (D–F). The minor repeat (ANGADDQPG) was observed 4 times among the 6 VK247 isolates. Sequence analysis showed that the terminal amino acid

sequence motifs were 100% concordant with GDRAAGQPA (VK210) and ANGAGNQPG (VK247) predicted by previously reported *P. vivax* strains (not shown here). Shared motif patterns were observed between VK210. No shared motif patterns were observed between VK247 infected people or regions. Sequence GenBank accession nos. EU031819–EU031836.

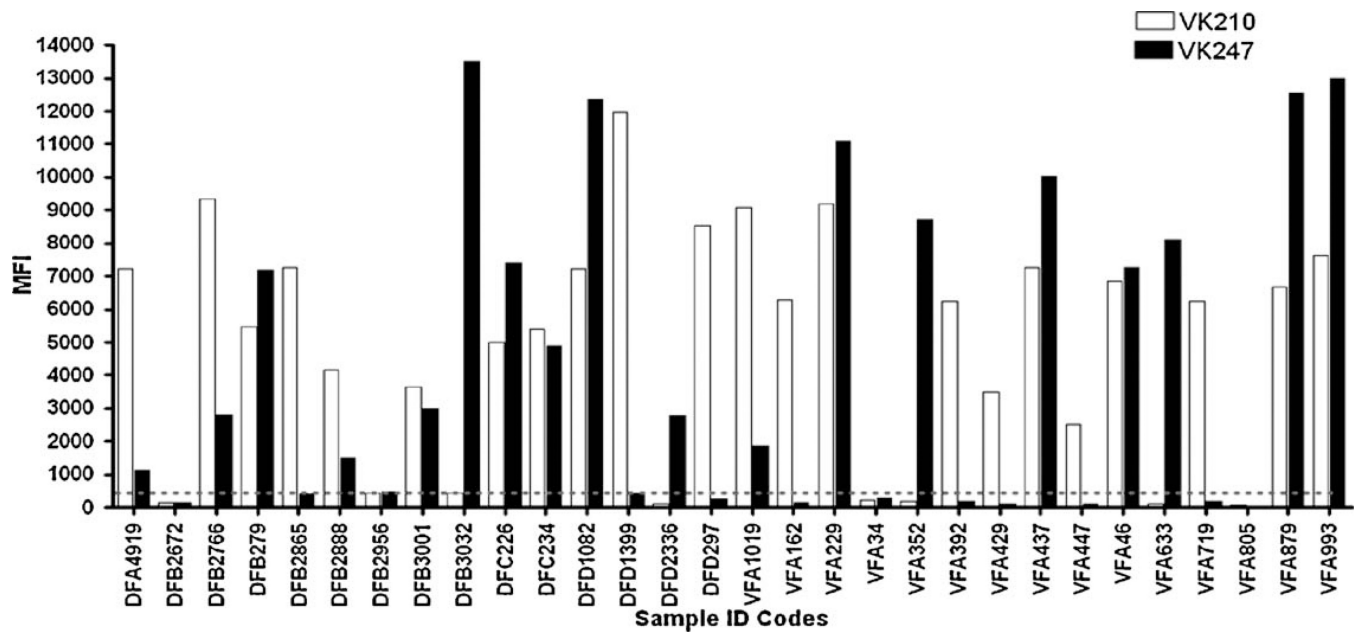


Fig. 4. Overview of *P. vivax* VK210 and VK247 strain infections in select Wosera and Mugil study participants. Strain specific fluorescence data shown as median fluorescence intensity (MFI) for VK210 (white) and VK247 (black). Select study participants ($n = 20$) were from villages in the Wosera (DFA, DFB, DFC, DFD; $n = 15$) and villages in Mugil (VFA; $n = 15$) study sites. LDR-FMA MFI values are found on the Y-axis and range from 0 to 14,000. A fluorescence value of approximately 500 (as shown by the grey dotted line) is the threshold for positivity and corrects for background activity. Samples chosen represent the infection status commonly observed in the two populations surveyed. Single infection with VK210 and VK247 are found as well as mixed infection with both variants and lack of *P. vivax* infection.

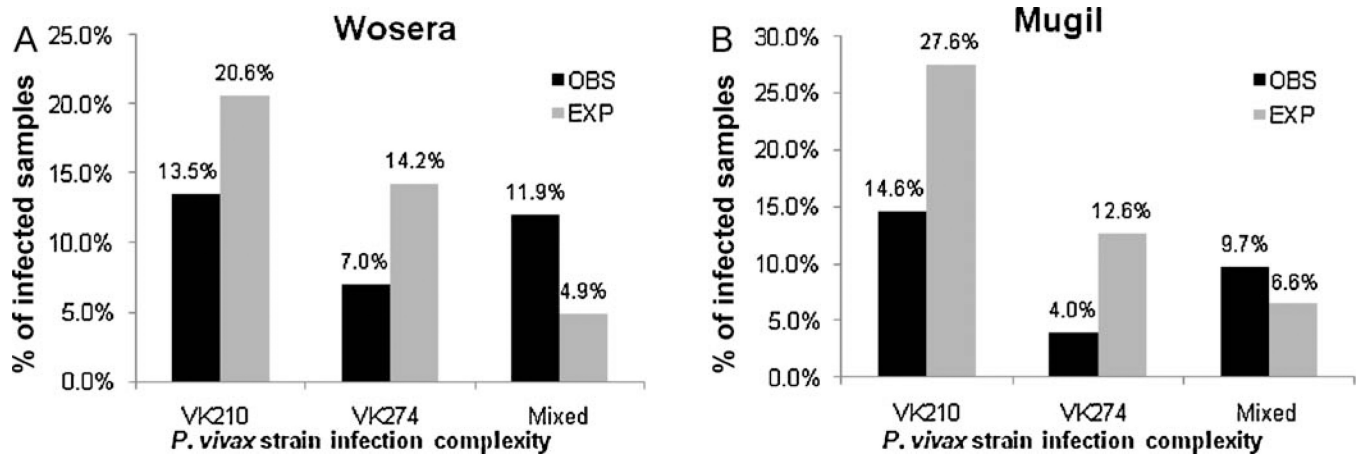


Fig. 5.

The prevalence and complexity of infection by *P. vivax* VK210 and VK247 for Wosera (a) and Mugil (b) study sites. Observed percentages (black) are based upon infection counts. Expected percentages (grey) are based upon a Multiple Kind Lottery strategy for predicting single- and mixed-strain infections. Chi-square analysis showed significant difference between the expected infection values and the observed infections (Wosera: $\chi^2 = 122.12, p > 0.001, 3$ degrees of freedom, Mugil: $\chi^2 = 197.68, p > 0.001, 3$ degrees of freedom).

Table 1Ligase detection reaction primers for genotyping *P. vivax* variants (VK210 and VK247).

| Variant | Primer sequence ^a | FlexMap™ microsphere set id no. ^b |
|-----------------|---|--|
| VK210-TAG | 5' cta caa aca aac aaa cat tat caa GGW GAY AGA GCA GMT GGA CAR CCA GCA 3' | 28 |
| VK210 conserved | 5' -/5Phos/GGA AAT GGT GCA GGT GGA CAG GCA GCA/3Bio/-3' | |
| VK247-TAG | 5' cta act aac aat aat cta act aac GCA AAT GGR GCN GGY AAT CAA CCA GGA 3' | 80 |
| VK247 conserved | 5' -/5Phos/GCA AAT GGT GCA GGT GGA CAG GCA GCA/3Bio/-3' | |

W= A or T; Y=T or C; M=A or C; R=G or A, N=A, T, C or G.

^aPrimers were designed using *pvcs* sequence for both subtypes: VK210 (GenBank accession number M11926), VK247 (GenBank accession number M28745). Lowercase nucleotides represent the TAG sequence specific to the FlexMap™ microsphere and are added to the 5' end of each variant-specific LDR primer.

^bID, identification. One hundred unique Luminex microsphere sets are synthesized to exhibit unique fluorescence. Each microsphere set is coupled to different anti-TAG sequences. Anti-TAG sequences are complementary to allele-specific TAG sequences.

Table 2

pvcsf Repeat motifs and post-repeat region nucleotide and amino acid sequences.

| PvCSP variant | Motifs | Post-repeat region | | | | | | | | | |
|-------------------------|---|--------------------|--|--|--|--|--|--|--|--|--|
| | | | | | | | | | | | |
| VK210 ^a | | | | | | | | | | | |
| Nucleotide ^b | GGH GAY AGW GCA SMT GGA CAR CCA GCW | | | | | | | | | | |
| Amino acid | G D R A D/A/PG Q P A | | | | | | | | | | |
| Terminal repeat | GGA GAT AGA GCA GCT GGA CAG CCA GCA GGA AAT GGT GCA GGT GGA CAG GCA GCA | | | | | | | | | | |
| VK247 ^c | G D R A A G Q P A G N G A G G G A A | | | | | | | | | | |
| Nucleotide ^b | GCA AAT GGD GCH GRY RAT CAA CCA GGA | | | | | | | | | | |
| Amino acid | A N G A G/D D/N Q P G | | | | | | | | | | |
| Terminal repeat | GCA AAT GGG GCA GGT AAT CAA CCM GGA GCA AAT GGA GCA GGT GGA CAG GCA GCA | | | | | | | | | | |
| | A N G A G N Q P G A N G A G G Q A A | | | | | | | | | | |

^aSequence data analyzed from GenBank accession nos. AY443700, AY443726, AY632243, AY632256, AY632288, AY632319, and M11926.

^bIn the nucleotide sequence H=A/C/T; Y=T/C; W=A/T; S=G/C; M=A/C; R=G/A; D=G/A/T.

^cSequence data analyzed from GenBank accession nos. AY632245, AY632318, AY632299, AY632316, and M28745.

Table 3

| | Vivax+ | Vivax- |
|--|--------|--------|
| (a) Wosera – <i>Plasmodium</i> specie ^a and <i>pvcsp</i> ^b concordance | | |
| <i>pvcsp</i> + | 168 | 60 |
| <i>pvcsp</i> - | 31 | 444 |
| <i>n</i> = 703 | | |
| (b) Mugil – <i>Plasmodium</i> specie ^a and <i>pvcsp</i> ^b concordance | | |
| <i>pvcsp</i> + | 200 | 79 |
| <i>pvcsp</i> - | 108 | 599 |
| <i>n</i> = 986 | | |

^a *P. vivax* positivity determined by previously described PCR LDR-FMA *Plasmodium* diagnostic tool (McNamara et al., 2006).

^b Samples giving a positive result for *pvcsp* variant VK210 and/or VK247 by the described PCR LDR-FMA method in this manuscript.

Table 4

Pvcsp distribution between Wosera and Mugil.^a

| | VK210 | VK247 |
|--------|-------------------------|------------|
| Wosera | 179(188.9) ^b | 134(121.3) |
| Mugil | 240(230.1) | 135(147.7) |

^aTotal number of samples evaluated between the two study sites=1689.

^bValues in parenthesis represent the expected infections.

Table 5

Summary of published *P. vivax* VK210 and VK247 from regional surveys.

| Author ^a | Year ^b | Location | Samples | VK210 ^c | VK247 ^c | Mix ^d | VK210% | VK247% |
|---------------------|-------------------|------------|---------|--------------------|--------------------|------------------|--------|--------|
| Kain | 1993 | Thailand | 171 | 65 | 48 | 58 | 53.7 | 46.3 |
| Cui | 2003 | Thailand | 90 | 69 | 1 | 20 | 80.9 | 19.1 |
| Imwong | 2005 | Thailand | 100 | 90 | 9 | 1 | 90.1 | 9.9 |
| Moon | 2008 | Myanmar | 116 | 86 | 2 | 28 | 79.2 | 20.8 |
| Kim | 2006 | India | 151 | 150 | 1 | 0 | 99.3 | 0.7 |
| Leclerc | 2004 | Azerbaijan | 36 | 36 | 0 | 0 | 100.0 | 0.0 |
| Zakeri | 2006 | Iran | 136 | 96 | 24 | 16 | 73.7 | 26.3 |
| Zakeri | 2009 | Pakistan | 187 | 179 | 5 | 3 | 95.8 | 4.2 |
| Zakeri | 2010 | Afganistan | 202 | 175 | 14 | 13 | 87.4 | 12.6 |
| Machado | 2000 | Brazil | 48 | 35 | 0 | 13 | 78.7 | 21.3 |
| Storti-Melo | 2008 | Brazil | 126 | 91 | 4 | 31 | 111 | 22.3 |
| Bonilla | 2006 | Guayana | 46 | 34 | 3 | 9 | 78.2 | 21.8 |
| Current study | | PNG | 507 | 239 | 88 | 180 | 61.0 | 39.0 |

^aManuscript details provided in text.

^bYear of publication.

^cSingle VK210 or Single VK247 infection.

^dInfection includes VK210 and VK247 *P. vivax* strains.